absorbance may easily mask this band because of its close proximity.

Voltammetry identified $Ni^{II/I}$ couples in all four complexes, with quasi-reversible behavior seen except for the case of IV, where the smaller cavity may be less appropriate for Ni^{I}, promoting irreversible behavior. It appears that the nickel(I) species are significantly more stable in aprotic solution than the nickel(III) species, from voltammetric behavior. However, the reverse appears to be the case in aqueous solution with no evidence of nickel(I) remaining ~ 100 μs after the pulse.

The nitro group electrochemistry of I and IV was also studied. While there have been several reports[30-32] of nitro group electrochemistry, electrochemical studies of nitro groups on coordinated ligands have appeared only recently.[26,33,34] In aqueous solution nitro groups are electrochemically reduced in two steps to hydroxylamine

$$-NO_2 \xrightarrow{2e^-,\,2H^+} -N{=}O \xrightarrow{2e^-,\,2H^+} -NHOH \qquad (2)$$

This appears as a single, four-electron wave usually and is clearly irreversible. This typical behavior was observed for I and IV in water, reduction occurring at -0.91 V versus Ag/AgCl in both cases. The redox behavior of the nitro group in acetonitrile was quite different. In the voltammograms of I and IV, two one-electron steps are observed near -1.1 V versus Ag/AgCl, and the process is irreversible. The aprotic conditions clearly make a mechanism such as eq 2 unreasonable, since a ready source of protons is not available. Only upon the addition of an anhydrous acid is a multielectron wave at a more positive potential observed. The two steps seen in acetonitrile presumably relate to reduction to a radical anion and then to a dianion. This has been observed in the nonaqueous electrochemistry of nitro aromatic compounds where delocalization of the negative charge is possible.[30] However, such a reaction on a saturated system would seem less likely at face value. It is possible that there is some metal-nitro anion interaction that acts to stabilize the radical via an axial metal orbital overlap with the pendant nitro group orbitals.

Conclusions

It is apparent that a pendant nitro group on a saturated ligand coordinated to Ni^{II} is an effective trap for e_{aq}, forming an intermediate with a nitro radical anion. In the absence of the nitro group, the Ni^{II} center is readily reduced by e_{aq} to its monovalent state. Rapid first-order decay processes operate in either case. With OH, the first observable species is a Ni^{III} compound in all cases studied, and this rapidly reacted by a first-order process. Both $Ni^{II/I}$ and $Ni^{II/III}$ processes were observed voltammetrically, but only in aprotic solution. The unusual tricyclic "football" structures in I-III did not appear to offer any added stabilization to either Ni^{I} or Ni^{III} complexes, when compared with other known compounds. However, there is clear evidence that the amine pendant on II can act to stabilize a Ni^{III} species, presumably by acting as an axial ligand for an octahedral ion.

Acknowledgment. Support from the Australian Institute of Nuclear Science and Engineering and from the Australian Research Grants Scheme is gratefully acknowledged.

(30) Bard, A. J.; Lund, H. *Encyclopedia of Electrochemistry of the Elements*; Dekker: New York, 1979; Vol. 13, p 77.
(31) Kokorekina, V. A.; Petrosyan, V.; Feoktistov, L. G. *Electrosint. Monomerov* **1980**, 83.
(32) Bond, A. M.; Lawrance, G. A.; Lay, P. A.; Sargeson, A. M. *Inorg. Chem.* **1983**, *22*, 2010.
(33) Gahan, L. R.; Lawrance, G. A.; Sargeson, A. M. *Inorg. Chem.* **1984**, *23*, 4369.
(34) Ziegerson, E.; Ginzburg, G.; Meyerstein, D.; Kirschenbaum, L. J. *J. Chem. Soc., Dalton Trans.* **1980**, 1243.

Contribution from the Exxon Research and Engineering Company, Annandale, New Jersey 08801

Transition-Metal Pteridine Complexes. Preparation and Characterization of Cobalt(II) Pteridines

Sharon J. Nieter Burgmayer† and Edward I. Stiefel*

Received March 23, 1988

The formation, isolation, and structural characterization of cobalt(II) pteridine complexes are described. The ligands are 4-oxopteridines with substituents at the 2-, 6-, and 7-positions of the pteridine core. Electronic and infrared spectral data on the series of complexes indicate that the pteridine ligands are coordinated to divalent cobalt via the oxygen atom in the 4-position and the pyrazine ring nitrogen in the 5-position. Two cobalt complexes of the chelate 2-(ethylthio)-4-oxopteridinate (ethp) have been structurally characterized by single-crystal X-ray diffraction. $Co(ethp)_2(H_2O)_2 \cdot 2DMF$ (DMF = *N*,*N*-dimethylformamide) crystallizes in the triclinic space group $P\bar{1}$ with cell dimensions $a = 7.468$ (3) Å, $b = 8.358$ (3) Å, $c = 12.309$ (4) Å, $\alpha = 101.46$ (2)°, $\beta = 94.44$ (2)°, and $\gamma = 101.93$ (2)° defining a volume of 731.1 (5) Å^3 for $Z = 1$. The cobalt atom sits on the crystallographic inversion center, placing the two pteridine chelates in a trans configuration and the aquo ligands in the remaining axial sites of a distorted octahedron. $Co(ethp)_2(imid)_2$ (imid = imidazole) crystallizes in the monoclinic space group $C2/c$ with cell parameters $a = 22.329$ (4) Å, $b = 16.096$ (3) Å, $c = 13.205$ (2) Å, and $\beta = 129.84°$ defining a volume of 3644 (1) Å^3 for $Z = 4$. The cobalt in this complex also has distorted-octahedral geometry, but the chelating pteridine ligands occupy cis positions, leaving two cis coordination sites for the imidazole ligands. The Co-N bond lengths to the pteridine ligands increased by 0.08 Å from the aquo to the imidazole complex, apparently resulting from imidazole coordination trans to this bond.

Pteridines are fused-ring nitrogen heterocyclic compounds that are ubiquitous in nature. They are found as the core structures of folic acid and flavin adenine dinucleotide (FAD) and function as cofactors for enzymes involved in hydroxylation[1] and methyl transfer,[2] as redox mediators,[3] and as pigments for eyes and wings in certain insects.[4] Variation of the substituents on the pteridine core of folates has provided a synthetic anticancer drug, methotrexate.[5] The majority of the naturally occurring pteridine compounds have the 2-amino-4-oxo substitution pattern on the

† Current address: Department of Chemistry, Bryn Mawr College, Bryn Mawr, PA 19010.

(1) Benkovic, S. J. *Annu. Rev. Biochem.* **1980**, *49*, 227.
(2) (a) Blakeley, R. L. *The Biochemistry of Folic Acid and Related Pteridines*; Elsevier: New York, 1969. (b) Van Beelen, P.; Van Neck, J. W.; de Cock, R. M.; Vogels, G. D.; Guijt, W.; Haasnoot, C. A. G. *Biochemistry* **1984**, *23*, 4448.
(3) Dolphin, D. *Adv. Chem. Ser.* **1980**, *No. 191*, 65.
(4) Pfleiderer, W. In *Biochemical and Clinical Aspects of Pteridines*; Wachter, H.; Curtius, H. C., Pfleiderer, W., Eds.; DeGruyter: Berlin, 1982.

0020-1669/88/1327-4059$01.50/0

Table I. Pteridine Ligands

ligand	abbrev[a]	structure
2-amino-6-(hydroxymethyl)-4-oxopteridine	HMP	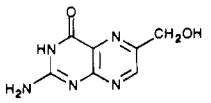
2-(ethylthio)-4-hydroxypteridine	ETHP	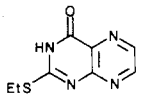
4-hydroxypteridine	HP	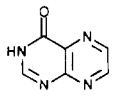
2,4-dioxopteridine (lumazine)	LUM	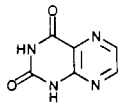
2-amino-6,7-dimethyl-4-hydroxypteridine	DMP	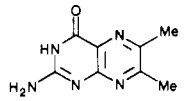
6,7-dimethyl-4-hydroxypteridine	HDMP	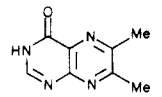

[a] Capital letters refer to the free pteridine; lower case letters designate the anionic ligand.

bicyclic core and have the trivial class name pterin. The pteridine and pterin core structures are shown in Table I. Fusion of a third benzene ring to a 2,4-dioxo-substituted pteridine group produces the core structure of the isoalloxazines, of which flavins are a subgroup. We have begun studies that seek to systematize the nature of transition-metal coordination to these molecules. Various reports exist in the literature for metal interaction with folates and pteridines,[6] flavins,[7] and isoalloxazines,[8] but only a few of these have dealt with well-characterized materials or used X-ray crystallography to confirm the chelation mode of the heterocyclic ligands. At this time, two pterin cofactors are known for enzymes that also require a metal for catalytic activity. Within the group of aromatic acid hydroxylases, phenylalanine hydroxylase (PAH) is known to require a pterin cofactor, tetrahydrobiopterin, and a first-row transition metal. PAH enzymes from mammalian sources utilize ferrous ion[9] while a bacterial PAH from *Chromobacterium violaceum* has recently been shown to require copper.[10] The molybdenum cofactor, Mo-co, found in approximately a dozen diverse enzymes, has a necessary pterin component whose structure has not yet been fully determined.[11]

The ability of Co(II) to bind pteridines and pterins is demonstrated in this work. While no enzyme is known to require cobalt and a pteridine for activity, we find that formation of pteridine complexes of this first-row transition metal is facile and the products do not require any special handling to protect them from decomposition in the atmosphere. This facilitates spectroscopic characterization as well as development of methods to solubilize complexes of these notoriously insoluble ligands. The preparations reported here have been successfully extended to the biologically relevant metal ions Fe(II), Fe(III), Cu(II), and Cu(I), and studies of these complexes are currently in progress.[12] A previous report has demonstrated the ability of molybdenum in a biologically relevant oxidation state to bind the pterin ligand.[13]

Experimental Section

The pteridine and pterin ligands used in this work were purchased from Aldrich Chemical Co. except for 6-hydroxymethylpterin, which was prepared for us by Barbara Nowak-Wydra and Alan Katritzky, University of Florida, Gainesville, FL. Cobalt nitrate and cobalt acetate were purchased from Alfa Ventron Products. Imidazole obtained from Aldrich Chemical Co. was recrystallized from methylene chloride and hexane before use. Infrared spectra of KBr disks were recorded on a Perkin-Elmer Model 683 instrument and are referenced to the 1601.2-cm^{-1} absorption of polystyrene. Microanalyses were performed by Galbraith Laboratories, Knoxville, TN. Analytical data are shown in Table II (supplementary material). Preliminary inspection of crystals for X-ray analysis was done at Exxon Research and Engineering Co., and the full structural analyses were completed by Dr. Cynthia Day of Crystalytics Co., Lincoln, NE. Electronic spectra were recorded with a Hewlett-Packard 4501 spectrophotometer. Solution conductivities were measured by using a Barnstead PM-70CB conductivity bridge equipped with a Yellow Springs Instruments 3403 dip cell. Magnetic susceptibilities were obtained by the Gouy method using $HgCo(SCN)_4$ as a calibrant.

Preparation of Cobalt(II) Pteridine Complexes. Two reaction methods, A and B, were used. Complexes $Co(ethp)_2(H_2O)_2$ and $Co(hmp)_2(H_2O)_5$·DMSO were prepared by both methods. All other complexes reported were prepared according to method A. Representative procedures are given for preparation of $Co(ethp)_2(H_2O)_2$ by both methods.

$Co(ethp)_2(H_2O)_2$. Method A. 2-(Ethylthio)-4-hydroxypteridine (ETHP, 4.0 mmol) was suspended in 40 mL of distilled H_2O in a beaker. KOH (2 N) was added dropwise until all the solid dissolved; the pH was approximately 11.5. The solution of the ligand was neutralized to pH 8 with a 1 N HCl solution. This addition must be done slowly to avoid precipitation of the water-insoluble neutral pteridine ligand. Cobalt nitrate (2 mmol) was dissolved in 5 mL of H_2O and then added dropwise to the yellow ligand solution. The solution darkened, and a bright yellow powder precipitated. Chilling the product mixture in an ice bath aided coagulation of the fine particles. The solid was isolated by filtration to give a 69% yield of crude $Co(ethp)_2(H_2O)_2$.

Method B. ETHP (1 mmol) was dissolved in 15 mL of DMF to give a pale yellow solution. Cobalt acetate (0.50 mmol) was dissolved in 5 mL of DMF. Slow addition of the cobalt solution to the ligand solution caused a color change to a more intense orange-yellow, and a flocculent yellow solid precipitated. The mixture was chilled in a freezer overnight prior to filtering. The yield of $Co(ethp)_2(H_2O)_2$ by this method was 93%.

$Co(ethp)_2(imid)_2$. To a solution of $Co(ethp)_2(H_2O)_2$ (0.030 mmol) in DMF (10 mL) was added 1.0 mmol of imidazole. The solution immediately became orange, and 5 volumes of diethyl ether was added to induce precipitation of the product. Orange crystals grew overnight to give a 70% yield of $Co(ethp)_2(imid)_2$.

$Co(hmp)_2(H_2O)_5$·DMSO. This complex can be prepared by the aqueous method A or preferably by method B employing the polar aprotic solvent dimethyl sulfoxide. The ligand 6-hydroxymethylpterin (1 mmol) was dissolved in warm (50–60 °C) DMSO (30 mL). Cobalt acetate was dissolved in DMSO (5 mL), and the solution was then slowly added to the ligand solution. No precipitate formed. Adding 3 volumes of THF and chilling the mixture overnight in the freezer induced precipitation of the product as pale yellow crystals. The isolated yield was 79%.

$Co(dmp)_2(H_2O)_x$, $Co(hp)_2(H_2O)_4$, $Co(lum)_2(H_2O)_3$, and $Co(hdmp)_2(H_2O)_x$ were prepared by using method A on a 1.0-mmol scale. Isolated yields of yellow solids were in the range 70–90%.

Crystal Structures of $Co(ethp)_2(H_2O)_2$·2DMF and $Co(ethp)_2(imid)_2$. Crystals of both complexes were grown by slow evaporation of DMF solutions. Solutions of $Co(ethp)_2(imid)_2$ contained excess imidazole. Both complexes gave crystals having a parallelepipedic habit. The di-

(5) (a) Blakely, R. L.; Cocco, L. *Biochemistry* **1985**, *24*, 4702, 4772. (b) *Pteridine Chemistry*; Pfleiderer, W., Taylor, E., Eds.; Pergamon: Oxford, England, 1964.
(6) (a) Albert, A. *Biochem. J.* **1950**, *47*, ix. (b) Vonderschmitt, D. J.; Scrimgeour, K. G. *Biochem. Biophys. Res. Commun.* **1967**, *28*, 302. (c) Jacobson, K. B.; Ferre, J.; Caton, J. E. *Bioorg. Chem.* **1985**, *13*, 296.
(7) (a) Hemmerich, P. *Helv. Chim. Acta* **1964**, *47*, 464. (b) Clarke, M. J.; Dowling, M. G.; Garafalo, A. R.; Brennan, T. F. *J. Am. Chem. Soc.* **1979**, *101*, 223. (c) Wade, T. D.; Fritchie, C. J. *J. Biol. Chem.* **1973**, *248*, 2337. (d) Selbin, J.; Sherrill, J.; Bigger, C. H. *Inorg. Chem.* **1974**, *14*, 1736. (e) Gallagher, B. J.; Riechel, T. L. *Inorg. Chim. Acta* **1982**, *66*, 73. (f) Sawyer, D. T.; Gerber, J. N.; Amos, L. W.; DeHayes, L. J. *J. Less-Common Met.* **1974**, *36*, 487.
(8) (a) Yu, M. W.; Fritchie, C. J. *J. Biol. Chem.* **1975**, *250*, 946. (b) Fritchie, C. J. *J. Biol. Chem.* **1973**, *248*, 7516.
(9) (a) Wallick, D. E.; Bloom, L. M.; Graffney, B. J.; Benkovic, S. J. *Biochemistry* **1984**, *23*, 1295. (b) Dix, T. A.; Bollag, G. E.; Domanico, P. L.; Benkovic, S. J. *Biochemistry*; **1985**, *24*, 2955.
(10) Pember, S. O.; Villafranca, J. J.; Benkovic, S. J. *Biochemistry*; **1986**, *25*, 6611.
(11) Johnson, J. L.; Hainline, B. E.; Rajagopalan, K. V. *J. Biol. Chem.* **1984**, *259*, 5414.
(12) Burgmayer, S. J. N.; Baruch, A.; Brodie, S.; Jafri, A.; Perkinson, J.; Yoon, K. Presented at the 195th National Meeting of the American Chemical Society, Toronto, Canada, June 1988; paper INOR 672; to be submitted for publication in *Inorg. Chem.*
(13) Burgmayer, S. J. N.; Stiefel, E. I. *J. Am. Chem. Soc.* **1986**, *108*, 8310.

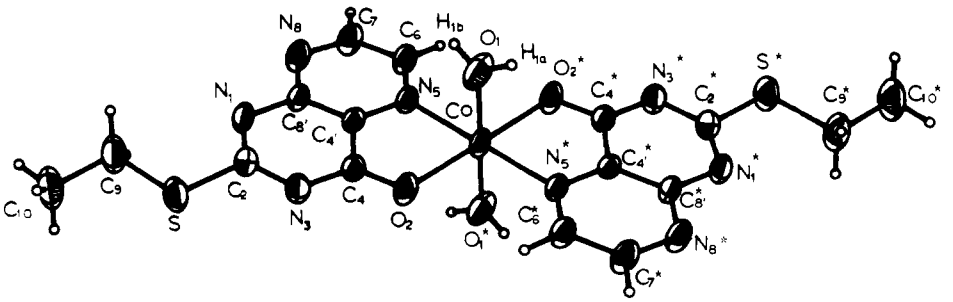

Figure 1. ORTEP drawing of $Co(ethp)_2(H_2O)_2 \cdot 2DMF$ showing the atomic numbering scheme. The thermal ellipsoids are drawn to encompass 50% electron density.

mensions of the orange-yellow crystal of $Co(ethp)_2(H_2O)_2 \cdot 2DMF$ were 0.2 × 0.4 × 0.5 mm, and the edge lengths of the orange crystal of $Co(ethp)_2(imid)_2$ were between 0.7 and 0.8 mm. Coating the crystals with epoxy caused degradation after several days. The X-ray analyses were performed on crystals sealed with a drop of mother liquor in thin-walled capillary tubes. X-ray data were collected at room temperature on a Nicolet automated diffractometer using molybdenum radiation and a graphite monochromator. The crystal of $Co(ethp)_2(H_2O)_2 \cdot 2DMF$ showed a slight twinning that necessitated use of a wide scan angle (2.20°) during data collection. The agreement between equivalent reflections was satisfactory as judged by merging R factor values of 0.0078 for $Co(ethp)_2(H_2O)_2 \cdot 2DMF$ and 0.0058 for $Co(ethp)_2(imid)_2$. Both structures were solved by direct methods using versions of Nicolet E-XTL and SHELXTL programs as modified by Crystalytics Co.[14]

Both crystals had molecules of DMF solvent in the lattice. The crystal of $Co(ethp)_2(H_2O)_2 \cdot 2DMF$ had well-ordered positions occupied by two DMF molecules per complex, but the crystal of $Co(ethp)_2(imid)_2$ had severely disordered DMF solvent molecules occupying several orientations in the lattice. The values listed for the molecular weight, calculated density, and linear absorption coefficient do not include the disordered solvent. Because of this severe disorder in the DMF solvate molecules, no distinction of carbon, nitrogen, and oxygen atoms could be made. These positions of electron density maxima observed in difference Fourier maps were arbitrarily assigned as carbon atoms. The six atoms C_{s1}–C_{s6} were included in the structure factor calculations with carbon scattering factors, and all except C_{s6} were assigned full occupancy (C_{s6} was assigned an occupancy factor of 0.50). Hydrogen atoms of the aquo ligands in $Co(ethp)_2(H_2O)_2 \cdot 2DMF$ were located from a difference Fourier synthesis and refined isotropically. All other hydrogen atom positions in this complex were calculated for a C–H distance of 0.96 Å and assigned fixed thermal parameters based on 1.2 times the equivalent isotropic thermal parameter of the atom to which it is bonded. Hydrogen atoms of the methyl groups in $Co(ethp)_2(imid)_2$ were located from a difference Fourier synthesis, and the methyl group was refined as a rigid rotor having C–H bond lengths of 0.96 Å. All other hydrogen atom positions were calculated at C–H and N–H bond distances of 0.96 and 0.93 Å, and thermal parameters were fixed as above. All hydrogen atoms were included in the structure factor calculation. Refinement of the extinction parameter was made in the final cycles to a value of 0.000 37. No absorption correction was made for either structure. Table III lists the parameters used in data collection and refinement.

Table III. Crystallographic Parameters: Data Collection and Structure Refinement

	$Co(ethp)_2(H_2O)_2 \cdot 2DMF$	$Co(ethp)_2(imid)_2$
mol formula	$CoS_2O_6N_{10}C_{22}H_{32}$	$CoS_2O_2N_{12}C_{22}H_{22}$
fw	655.6	609.5
space group	triclinic, $P\bar{1}$ (No. 2)	monoclinic, $C2/c$ (No. 15)
a, Å	7.468 (3)	22.329 (4)
b, Å	8.358 (3)	16.096 (3)
c, Å	12.309 (4)	13.205 (2)
α, deg	101.46 (2)	
β, deg	94.44 (2)	129.84 (1)
γ, deg	101.93 (2)	
V, Å^3	731.1 (5)	3644 (1)
Z	1	4
density(calcd), g/cm^3	1.489	1.110
density(measd), g/cm^3	1.489	1.060
μ, mm^{-1}	0.77	0.61
radiation	λ(Mo Kα) = 0.710 73 Å	
scan range, deg	$3.0 < 2\theta < 50.7$	$3.0 < 2\theta < 50.7$
octants collected	$\pm h,\pm k,+l$	$\pm h,+k,+l$
scan width, deg	2.20	1.40
bkgd	25% of full peak width on each side	
no. of unique data	2658	3323
no. of data with $I > 3\sigma(I)$	1869	2281
no. of variables	205	231
R (R_w)	0.033 (0.033)	0.048 (0.052)
largest peak in final diff map, e/Å^3	0.33	0.33
goodness of fit	1.62	2.63

Results and Discussion

Syntheses. The synthesis of cobalt pteridine and pterin complexes is easily accomplished in aqueous or polar aprotic solution. Table I lists the pteridines used in this study together with the abbreviations. All the pteridines react in a similar manner with cobalt nitrate in alkaline aqueous solutions to produce yellow products. Elemental analyses listed in Table II (supplementary material) show that each complex is a bis chelate having varying amounts of hydration and solvation. The materials prepared by this method are not easily redissolved, presumably due to the strong hydrogen bonding possible within the hydrated solids. A second method of preparation was devised wherein the substitution of a highly polar but aprotic solvent for water produces materials having the same cobalt/pteridine stoichiometry that are more easily redissolved for purification and crystallization. Complexes of the 2-(ethylthio)pteridine ligand ETHP are the most readily solubilized and can be redissolved in DMF or DMSO. The cobalt complexes of HMP and HP are soluble in DMSO only, and the lumazine complex is only slightly soluble in this solvent. The reaction of cobalt nitrate with lumazine in aqueous solution had been reported earlier by Goodgame and Schmidt.[15] They postulated that the anionic lumazine ligand coordinated through the N_1 or N_3 of the pyrimidine ring. We give proof that the mode of coordination in all the cobalt(II) complexes of pteridines is through O_4 and N_5 (vide infra). Our observations show that cobalt acetate deprotonates pteridines and that the resultant pteridinate ions chelate cobalt and displace acetate in solvents less polar than water. In contrast, Goodgame and Schmidt found that first-row transition-metal halides in dimethoxypropane/methanol mixtures did not deprotonate lumazine and displace the halide.

Addition of imidazole to DMF solutions of $Co(ethp)_2(H_2O)_2$ causes an immediate color change from yellow to orange, indicating facile reactivity of the Co(II) ion. Elemental and X-ray

(14) (a) Scattering factors are taken from: Cromer, D. T.; Waber, J. T. In *International Tables for X-ray Crystallography*; Ibers, J. A., Hamilton, W., Eds.; Kynoch: Birmingham, England, 1974; Vol. IV. (b) $I = S(C + RB)$ and $\sigma^2(I) = C + R^2B$, where I = intensity, C = total integrated peak count, R = ratio of scan count time to background count time, and B = total background count time. (c) The weighting scheme used in the least-squares minimization of the function was $\sum w(|F_o| - |F_c|)^2$, where $w = 1/\sigma(F_o)^2$ and $\sigma(F_o) = [\sigma^2(F_o) + \rho^2F_o^2]^{1/2}$ with ρ assigned a value of 0.01. Expressions for the residuals are $R = \sum||F_o| - |F_c||/\sum|F_o|$ and $R_w = [\sum w(|F_o| - |F_c|)^2/\sum w(F_o)^2]^{1/2}$. (d) The "goodness of fit" is GOF = $\{\sum w(|F_o| - |F_c|)^2/(NO - NV)\}^{1/2}$, where NO is the number of observations and NV is the number of variables. (e) The anisotropic thermal parameter is of the form $\exp[-0.25(B_{11}h^2a^{*2} + B_{22}k^2b^{*2} + B_{33}l^2c^{*2} + 2B_{12}hka^*b^* + 2B_{13}hla^*c^* + 2B_{23}klb^*c^*)]$.

(15) Goodgame, M.; Schmidt, M. A. *Inorg. Chim. Acta* **1979**, *36*, 151.

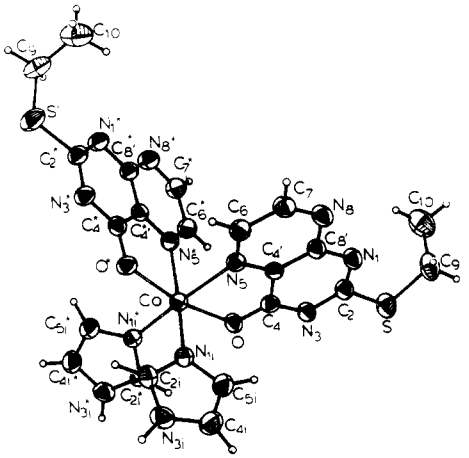

Figure 2. ORTEP drawing of $Co(ethp)_2(imid)_2$ showing the atomic numbering scheme. Thermal ellipsoids are drawn to concompass 50% electron density.

analyses (see below) show that the two aquo ligands have been substituted by two imidazole ligands. Addition of imidazole to other cobalt pteridine complexes did not give the same result and often appeared to cause precipitation of the free ligand, presumably by protonation of the pteridine ligand.

Magnetic susceptibilities of powdered samples of $Co(ethp)_2(H_2O)_2$ and $Co(ethp)_2(imid)_2$ were measured at room temperature. The values of μ_{eff} obtained ($Co(ethp)_2(H_2O)_2$, 6.2 μ_B; $Co(ethp)_2(imid)_2$, 5.7 μ_B) are typical of high-spin octahedral Co(II) centers.[16]

Structures of $Co(ethp)_2(H_2O)_2 \cdot 2DMF$ and $Co(ethp)_2(imid)_2$. Two cobalt complexes of 2-(ethylthio)-4-hydroxypteridine have been structurally characterized by single-crystal X-ray diffraction studies to verify the chelation mode of the ligands. Table III lists the crystallographic parameters used in data collection and refinement for each molecule. The atomic positions and thermal parameters for the two complexes are collected in Tables IV and V. ORTEP drawings of the aquo and imidazole complexes are shown in Figures 1 and 2, respectively.

The aquo complex adopts approximate C_{2h} symmetry, allowing the cobalt atoms to occupy the inversion centers in the crystal lattice. The two chelating ligands and the two aquo ligands are related by crystallographic symmetry. The two trans pteridine ligands form a planar girdle around the metal. The two axial sites are occupied by aquo ligands. The structure determination shows chelation of the pteridine unit through the exocyclic oxygen atom (O_2 in Figure 1) and a pyrazine ring nitrogen atom (N_5). This O_2,N_5-coordination of the pteridine unit is the same chelation mode observed in $Co(ethp)_2(imid)_2$ and in metal complexes of flavins and isoalloxazines.[7b,c,8]

Intramolecular bond angles and distances are tabulated for $Co(ethp)_2(H_2O)_2$ in Table VI. Angles in the inner coordination sphere about the cobalt atom are all near 90° and define a distorted-octahedral geometry. The angle having the largest deviation from the ideal 90° value is the pteridine chelate bite angle. This 80° bite angle is typical of a five-membered chelate ring with oxygen and nitrogen donor atoms in a delocalized system.[17] Bond angles within the pteridine unit are unchanged compared to those in other structures determined for pteridine molecules and flavin complexes.[7,8] The atoms of the pteridine core, including the sulfur atom of the ethylthio substituent, are coplanar, and the largest deviation from the idealized plane is less than 0.03 Å. Bond distances from coordinated oxygen and nitrogen atoms to the cobalt atom are normal for Co(II) complexes. In a comparison of structural details of $Co(ethp)_2(H_2O)_2$ to those of diaquobis(isoalloxazinato)copper(II),[8b] the Co^{II} atom has a shorter bond to N_5 (2.100 (2) versus 2.414 (2) Å for Cu–N_5) and has a similar

(16) Drago, R. S. *Physical Methods in Chemistry*; W. B. Saunders: Philadelphia, **1977**; p 426.
(17) O'Connor, C. J.; Sinn, E. *Inorg. Chem.* **1981**, *20*, 545.

Table IV. Atomic Coordinates and Isotropic and Anistropic Thermal Parameters for Non-Hydrogen Atoms in Crystalline $Co(SON_4C_8H_7)_2(OH)_2 \cdot 2OCHN(CH_3)_2$

(a) Atomic Coordinates and Isotropic Thermal Parameters

atom type[b]	fractional coord 10^4x	10^4y	10^4z	equiv isotropic thermal param, B, Å^2 × 10[c]
	Coordination Sphere			
Co	0[d]	0[d]	0[d]	28 (1)
S	3013 (1)	7581 (1)	3295 (1)	41 (1)
O_1	1362 (3)	999 (2)	−1222 (2)	42 (1)
O_2	1802 (3)	1827 (2)	1230 (2)	35 (1)
N_1	−51 (3)	6135 (2)	1873 (2)	28 (1)
C_2	1524 (4)	5917 (3)	2330 (2)	28 (1)
N_3	2239 (3)	4547 (3)	2174 (2)	30 (1)
C_4	1269 (4)	3179 (3)	1450 (2)	25 (1)
$C_{4'}$	−503 (3)	3259 (3)	904 (2)	22 (1)
N_5	−1503 (3)	1881 (2)	178 (2)	25 (1)
C_6	−3129 (4)	1975 (3)	−284 (2)	29 (1)
C_7	−3728 (4)	3470 (3)	−18 (3)	35 (1)
N_8	−2758 (3)	4844 (3)	678 (2)	33 (1)
$C_{8'}$	−1101 (4)	4746 (3)	1155 (2)	24 (1)
C_9	1831 (5)	9272 (4)	3419 (3)	47 (1)
C_{10}	2778 (5)	10659 (4)	4407 (3)	57 (1)
	Dimethylformamide Molecule of Crystallization			
O_{s1}	3743 (3)	−723 (3)	−2191 (2)	54 (1)
C_{s1}	3984 (4)	−2112 (4)	−2574 (3)	42 (1)
N_{s1}	2859 (3)	−3280 (3)	−3351 (2)	39 (1)
C_{s2}	3288 (6)	−4880 (4)	−3763 (4)	63 (1)
C_{s3}	1177 (5)	−2956 (5)	−3831 (3)	55 (1)

(b) Anisotropic Thermal Parameters[a,e]

atom type[b]	anisotropic thermal param, Å^2 × 10 B_{11}	B_{22}	B_{33}	B_{12}	B_{13}	B_{23}
	Coordination Sphere					
Co	28 (1)	17 (1)	37 (1)	12 (1)	−6 (1)	−1 (1)
S	43 (1)	24 (1)	45 (1)	7 (1)	−13 (1)	−6 (1)
O_1	52 (1)	29 (1)	53 (1)	21 (1)	11 (1)	14 (1)
O_2	33 (1)	23 (1)	46 (1)	17 (1)	−11 (1)	−1 (1)
N_1	30 (1)	17 (1)	34 (1)	7 (1)	−1 (1)	1 (1)
C_2	32 (1)	20 (1)	29 (1)	4 (1)	2 (1)	3 (1)
N_3	28 (1)	23 (1)	35 (1)	8 (1)	−6 (1)	0 (1)
C_4	26 (1)	20 (1)	28 (1)	7 (1)	−3 (1)	2 (1)
$C_{4'}$	23 (1)	19 (1)	25 (1)	8 (1)	1 (1)	5 (1)
N_5	25 (1)	18 (1)	31 (1)	9 (1)	−2 (1)	3 (1)
C_6	25 (1)	21 (1)	40 (1)	7 (1)	−7 (1)	3 (1)
C_7	28 (1)	27 (1)	50 (2)	14 (1)	−7 (1)	4 (1)
N_8	29 (1)	23 (1)	46 (1)	13 (1)	−4 (1)	4 (1)
$C_{8'}$	28 (1)	17 (1)	29 (1)	8 (1)	3 (1)	5 (1)
C_9	51 (2)	26 (1)	55 (2)	11 (1)	−13 (2)	−7 (1)
C_{10}	66 (2)	31 (1)	61 (2)	13 (1)	−12 (2)	−13 (1)
	Dimethylformamide Molecule of Crystallization					
O_{s1}	44 (1)	43 (1)	69 (2)	9 (1)	9 (1)	−7 (1)
C_{s1}	34 (1)	46 (2)	47 (2)	13 (1)	7 (1)	5 (1)
N_{s1}	33 (1)	39 (1)	42 (1)	8 (1)	3 (1)	2 (1)
C_{s2}	64 (2)	41 (2)	77 (3)	14 (2)	14 (2)	−7 (2)
C_{s3}	41 (2)	71 (2)	53 (2)	10 (2)	−1 (2)	19 (2)

[a] The numbers in parentheses are the estimated standard deviations in the last significant digit. [b] Atoms are labeled in agreement with Figure 1. [c] This is one-third of the trace of the orthogonalized B_{ij} tensor. [d] This is a symmetry-required value and is therefore listed without an estimated standard deviation. [e] The form of the anisotropic thermal parameter is given in ref 13e.

Co–O_2 bond distance (2.097 (4) versus 2.040 (2) Å for Cu–O). A comparison of C–C, C–N, and C–O bond distances between $Co(ethp)_2(H_2O)_2$ or $Co(ethp)_2(imid)_2$ and Cu^{II}(isoalloxazinato)$_2(H_2O_2)$ shows no significant differences. However, the O_2–C_4 distance in $Co(ethp)_2(H_2O)_2$ is shorter than the analogous bond length in the molybdenum–pterin complex $[Mo_2O_5(xanthopterinato)_2]^{2-}$ (1.261 (3) versus 1.303 (9) Å, respectively).[13] This result suggests that less electron density has been shifted from the carbonyl double bond to the oxygen atom upon pteridine complexation by this soft divalent metal as com-

Table V. Atomic Coordinates and Isotropic and Anisotropic Thermal Parameters for Non-Hydrogen Atoms in Crystalline $Co(SON_4C_8H_7)_2(N_2C_3H_4)_2$[a]

(a) Atomic Coordinates and Isotropic Thermal Parameters

atom type[b]	fractional coord 10^4x	10^4y	10^4z	equiv isotropic thermal param, B, Å^2 × 10[c]
		Coordination Sphere		
Co	0[d]	1223 (1)	2500[d]	40 (1)
S	2418 (1)	2924 (1)	1727 (1)	65 (1)
O	551 (1)	1356 (1)	1689 (2)	45 (1)
N_1	2123 (2)	3261 (2)	3340 (3)	48 (2)
C_2	1943 (2)	2777 (2)	2369 (4)	46 (2)
N_3	1438 (2)	2135 (2)	1777 (3)	44 (2)
C_4	1042 (2)	1940 (2)	2194 (3)	40 (2)
$C_{4'}$	1206 (2)	2426 (2)	3269 (3)	37 (2)
N_5	819 (2)	2226 (2)	3693 (3)	41 (2)
C_6	984 (2)	2673 (2)	4680 (4)	47 (2)
C_7	1532 (2)	3321 (2)	5220 (4)	53 (2)
N_8	1912 (2)	3531 (2)	4821 (3)	51 (2)
$C_{8'}$	1745 (2)	3072 (2)	3802 (3)	41 (2)
C_9	2943 (3)	3880 (3)	2482 (4)	70 (3)
C_{10}	2441 (3)	4639 (3)	1841 (5)	90 (4)
N_{1i}	770 (2)	326 (2)	3869 (3)	44 (2)
C_{2i}	604 (2)	−257 (2)	4351 (4)	51 (2)
N_{3i}	1204 (2)	−784 (2)	5108 (3)	55 (2)
C_{4i}	1785 (2)	−527 (3)	5127 (4)	62 (3)
C_{5i}	1515 (2)	156 (2)	4372 (4)	56 (2)
		Solvent[e]		
C_{s1}	−97 (7)	6434 (15)	737 (13)	344 (12)
C_{s2}	1228 (4)	5953 (10)	2511 (11)	262 (9)
C_{s3}	330 (11)	5400 (7)	1713 (19)	346 (23)
C_{s4}	0[d]	4726 (10)	2500[d]	388 (21)
C_{s5}	312 (12)	7531 (7)	2447 (19)	262 (19)
C_{s6}	475 (18)	6781 (21)	1860 (54)	359 (46)

(b) Anisotropic Thermal Parameters[a,f]

atom type[b]	anisotropic thermal param, Å^2 × 10 B_{11}	B_{22}	B_{33}	B_{12}	B_{13}	B_{23}
Co	46 (1)	35 (1)	50 (1)	0[d]	36 (1)	0[d]
S	79 (1)	72 (1)	77 (1)	−19 (1)	65 (1)	−13 (1)
O	52 (1)	41 (1)	53 (1)	−11 (1)	39 (1)	−12 (1)
N_1	56 (2)	46 (1)	54 (2)	−11 (1)	41 (1)	−7 (1)
C_2	50 (2)	47 (2)	51 (2)	−5 (2)	37 (2)	−1 (2)
N_3	54 (2)	44 (1)	50 (2)	−8 (1)	39 (1)	−7 (1)
C_4	45 (2)	39 (2)	41 (2)	4 (1)	31 (2)	1 (1)
$C_{4'}$	43 (2)	33 (1)	41 (2)	2 (1)	30 (1)	−0 (1)
N_5	48 (1)	38 (1)	47 (1)	1 (1)	36 (1)	−1 (1)
C_6	57 (2)	47 (2)	51 (2)	−1 (2)	41 (2)	−2 (2)
C_7	66 (2)	50 (2)	58 (2)	−8 (2)	47 (2)	−14 (2)
N_8	65 (2)	46 (2)	56 (2)	−13 (1)	45 (2)	−15 (1)
$C_{8'}$	44 (2)	40 (2)	44 (2)	−2 (1)	30 (2)	−1 (1)
C_9	77 (3)	80 (3)	74 (3)	−25 (2)	58 (2)	−5 (2)
C_{10}	119 (4)	74 (3)	91 (4)	−16 (3)	74 (3)	3 (3)
N_{1i}	49 (1)	40 (1)	54 (2)	0 (1)	38 (1)	3 (1)
C_{2i}	54 (2)	48 (2)	61 (2)	−6 (2)	42 (2)	2 (2)
N_{3i}	70 (2)	45 (2)	60 (2)	7 (1)	46 (2)	13 (1)
C_{4i}	57 (2)	63 (2)	75 (3)	14 (2)	46 (2)	18 (2)
C_{5i}	55 (2)	55 (2)	69 (2)	4 (2)	45 (2)	11 (2)

[a] The numbers in parentheses are the estimated standard deviations in the last significant digit. [b] Atoms are labeled in agreement with Figure 2. [c] This is one-third of the trace of the orthogonalized $\mathbf{B}_{ij}$ tensor. [d] This is a symmetry-required value and is therefore listed without an estimated standard deviation. [e] Solvent atoms C_{s1}–C_{s6} were located from difference Fourier syntheses and presumably correspond to average (disordered) positions for dimethylformamide molecules, which adopt several orientations in the lattice; all six atoms were included in the structure factor calculations with carbon scattering factors, and all except C_{s6} were assigned their normal full occupancy factors (C_{s6} was assigned an occupancy factor of 0.50). [f] The form of the anisotropic thermal parameter is given in ref 13e.

pared to pteridine complexation by the more electrophilic Mo(VI) ion.

The two DMF solvent molecules in the crystal lattice appear to occupy specific positions in order to maximize hydrogen bonding to protons of the aquo ligands. This interaction is illustrated in the drawing of the packing diagram given in Figure 3. Hydrogen-bonding distances between the carbonyl oxygens of DMF and aquo ligands (1.80 (3) Å for O_1–O_{s1}) are in the range acceptable for such interactions. The plane formed by the atoms of the DMF molecule has a dihedral angle of 4.2° to the plane of the pteridine atoms at an average distance of 3.4 Å.

Table VI. Bond Lengths (Å) and Angles (deg) in Crystalline $Co(SON_4C_8H_7)_2(OH_2)_2\cdot 2OCHN(CH_3)_2$[a,b]

		Distances	
Co–O_1	2.092 (2)	S–C_2	1.755 (2)
Co–O_2	2.086 (2)		
		S–C_9	1.803 (4)
Co–N_5	2.100 (2)		
		O_2–C_4	1.261 (3)
N_1–C_2	1.326 (4)		
N_1–$C_{8'}$	1.361 (3)	C_4–$C_{4'}$	1.457 (4)
N_3–C_2	1.347 (4)	$C_{4'}$–$C_{8'}$	1.392 (4)
N_3–C_4	1.334 (3)	C_6–C_7	1.400 (4)
N_5–$C_{4'}$	1.348 (3)		
N_5–C_6	1.324 (3)	C_9–C_{10}	1.513 (4)
N_8–C_7	1.321 (3)		
N_8–$C_{8'}$	1.353 (4)	O_1–H_{1a}	0.75 (4)
		O_1–H_{1b}	0.94 (4)
		Angles	
O_1–Co–O_1*[c]	180.0 (-)[d]	C_2–S–C_9	104.4 (1)
O_2–Co–O_2*[c]	180.0 (-)[d]		
N_5–Co–N_5*[c]	180.0 (-)[d]	Co–O_2–C_4	112.5 (2)
O_1–Co–O_2	89.3 (1)		
O_1–Co–N_5	90.1 (1)		
O_1–Co–O_2*[c]	90.7 (1)		
O_1–Co–N_5*[c]	89.9 (1)		
O_2–Co–N_5	80.7 (1)	Co–$N_5C_{4'}$	109.1 (2)
O_2–Co–N_5*[c]	99.3 (1)	Co–N_5–C_6	133.7 (2)

[a] The numbers in parentheses are the estimated standard deviations in the last significant digit. [b] Atoms are labeled in agreement with Figure 1. [c] Atoms labeled with an asterisk are related to those without by the crystallographic inversion center at (0, 0, 0) in the unit cell. [d] This is a symmetry-required value and is therefore listed without an estimated standard deviation.

Table VII. Bond Lengths (Å) and Angles (deg) in Crystalline $Co(SON_4C_8H_7)_2(N_2C_3H_4)_2$[a,b]

		Distances	
Co–O	2.097 (4)	S–C_2	1.748 (6)
Co–N_5	2.178 (2)	S–C_9	1.800 (5)
Co–N_{1i}	2.081 (2)		
		O–C_4	1.262 (4)
N_1–C_2	1.323 (6)		
N_1–$C_{8'}$	1.355 (7)	C_4–$C_{4'}$	1.447 (6)
N_3–C_2	1.350 (4)	$C_{4'}$–$C_{8'}$	1.393 (5)
N_3–C_4	1.344 (7)	C_6–C_7	1.406 (5)
N_5–$C_{4'}$	1.336 (7)		
N_5–C_6	1.317 (6)	C_9–C_{10}	1.500 (7)
N_8–C_7	1.298 (8)		
N_8–$C_{8'}$	1.361 (6)		
N_{1i}–C_{2i}	1.313 (6)	C_{4i}–C_{5i}	1.340 (6)
N_{1i}–C_{5i}	1.366 (6)		
N_{3i}–C_{2i}	1.340 (4)		
N_{3i}–C_{4i}	1.347 (7)		
		Angles	
O–Co–O*[c]	168.4 (1)	C_2–S–C_9	103.2 (3)
N_{1i}–Co–N_5*[c]	170.7 (2)		
O–Co–N_{1i}	94.9 (1)	Co–O–C_4	113.6 (3)
O–Co–N_5*[c]	92.9 (1)		
N_5–Co–N_{1i}	92.4 (1)		
N_{1i}–Co–O*[c]	93.2 (1)		
N_5–Co–N_5*[c]	84.3 (1)		
N_5–Co–O	78.4 (1)	Co–N_5–$C_{4'}$	110.1 (2)
N_{1i}–Co–N_{1i}*[c]	92.1 (1)	Co–N_5–C_6	133.9 (3)

[a] The numbers in parentheses are the estimated standard deviations in the last significant digit. [b] Atoms are labeled in agreement with Figure 2. [c] Atoms labeled with an asterisk are related to those without an asterisk by the symmetry operation $-x, y, {}^1/_2 - z$, where the fractional atomic coordinates (x, y, z) are given in Table V.

Table VIII. Infrared Data (cm^{-1}) for Pteridines and Their Co(II) Complexes

	ν_{NH}, ν_{OH}	$\nu_{C=O}$	$\nu_{C=O}$, $\nu_{N=N}$, $\nu_{C=N}$	other
ETHP	3180 w	1690 vs	1576 s	1330 m
			1539 s	1300 m
			1491 m	1228 s
			1456 m	1130 m
			1390 vs	1050 m
				960 m
$Co(ethp)_2(H_2O)_2$·2DMF	3330 vs	1650 vs[a]	1583 vs	1344 s
			1524 vs	1315 m
			1495 vs	1278 s
			1415 vs	1260 s
				1150 s
				1045 m
				960 m
$Co(ethp)_2(H_2O)_2$·H_2O	3330 vs	...	1589 vs	1344 s
			1520, 1500 vs	1280 s
			1423 sh, 1409 vs	1260 s
				1142 s
				1049, 1024 m
				964 m
$Co(ethp)_2(imid)_2$	3120[b]	...	1579 vs	1340 s
			1520 sh, 1500 vs	1279 s
			1409 vs	1258 s
				1150 s
				1072 s[b]
				1048 m
				962 m
DMP	3260 s	1728 m	1637 m	1362 m
	3070	1685 vs	1543 m	1283 m
			1515 m	1260 m
			1471 m	1079 m
			1390 s	
$Co(dmp)_2(H_2O)_x$	3440 s	...	1639 vs	1345 s
	3280 s		1589 vs	1233 s
	3140 s		1521 vs	1092 m
			1455, 1430 vs	1000 m
			1390 s	
HMP	3260 s	1720 sh	1617 m	1365 m
	3100 s	1688 vs	1529 m	1290 m
			1490 m	1240 m
			1410 m	1167 m
				1127 m
				1078 m
$Co(hmp)_2(H_2O)_5$·DMSO	3420 s	...	1629 vs	1350 s
	3360 s		1591 vs	1227 m
	3190 s		1534, 1520 vs	1175 m
			1450 vs	1061 m
				1029 m
HP	3400 s	1715 vs	1614 vs	1343 s
		1701 vs	1591 vs	1319 m
			1549 vs	1229 m
			1467 m	1219 m
			1397, 1373 m	
$Co(hp)_2(H_2O)_4$	3580 w	...	1589 vs	1345 vs
	3080 vs		1541	1261 s
			1516 vs	1183 m
			1484 s	1131 vs
LUM	3170	1720 vs	1554 vs	1300 m
	3080	1698 vs	1390 vs	1277 m
				1218 s
				1185 m
				1070 m
				1031 m
$Co(lum)_2(H_2O)_3$	3300 vs	1652 vs	1620 vs	1309 vs
			1575 vs	1290 vs
			1530 s	1230 vs
			1501 vs	1164 m
			1415 vs	1069 m
HDMP	3200 vs	1710 vs	1600 vs	1368 s
			1555 vs	1275 s
			1455 s	1254 vs
			1390 vs	
$Co(hdmp)_2(H_2O)_x$	3240 vs	...	1641 m	1358 s
			1583 vs	1318 vs
			1550 vs	1231 s
			1512 vs	
			1470 s	
			1391, 1375 s	
xanthopterin	3330 s	1682 vs	1590 vs	
	3270 s	1655 vs	1400 m	
$[Mo_2O_5(xanthopterin)_2]^{2-}$	3460	...	1618 s	
	3340 s		1575 vs	
	3200 s		1540 vs	
			1475 m	
			1438, 1421 vs	

[a] Carbonyl stretch from DMF. [b] Vibration from imidazole ligand.

Substitution of two imidazole molecules for water ligands in the coordination sphere of the Co(II)–bis(pteridine) moiety produces a crystalline solid where the disposition of the two pteridine ligands has changed from trans to cis as illustrated by the ORTEP drawing of $Co(ethp)_2(imid)_2$ given in Figure 2. The coordinated oxygen atoms of the pteridine ligand remain trans to each other, but the coordinated nitrogen atoms of the pteridine chelate are now each trans to a nitrogen atom of an imidazole group. This complex possesses crystallographic C_2 symmetry with the 2-fold axis passing between the pteridine ligands, through the cobalt atom, and between the imidazole ligands. The octahedral geometry about the cobalt atom is distorted with the pteridine chelate again responsible for the distortion from ideal geometry. Angles and bond distances within the pteridine ligand given in Table VII for this complex do not differ significantly from those in $Co(ethp)_2(H_2O)_2$·2DMF discussed above.

Comparing the bond lengths of atoms coordinated to Co(II) in the two Co structures reported in this work indicates an outcome of, and perhaps the reason for, the pteridine rearrangement. While the Co(II)–O(pteridine) distances are virtually identical in the two complexes, the Co(II)–N_5 bond length has increased by nearly 0.08 Å from 2.100 (2) to 2.178 (2) Å in going from the aquo to the imidazole complex. Of the two types of Co(II)–N bonds in the latter complex, the imidazole appears to form the stronger bond as its coordinated nitrogen atom sits nearly 0.1 Å closer to the metal atom. The observed rearrangement of the chelate ligands to a cis orientation may occur to improve bonding interactions between the cobalt atom and the cis imidazole ligands as compared to the hypothetical trans imidazole structure. The effect of trans imidazole groups bound to Co(II) on bond strength is shown by the structure of Co(L-histidine)$_2$, where Co(II)–N_{imid} = 2.18 Å.[18] In $Co(ethp)_2(imid)_2$ the dihedral angle between the plane of the imidazole and the plane formed by O, N_5*, O*, and N_{imid} is 29.6°. The packing diagram shown in Figure 4 indicates that stacking interactions between planar pteridine ligands and imidazole rings stabilize the crystal lattice.

Spectral Properties of Cobalt Pteridine Complexes. The cobalt complexes prepared in this study were investigated by using infrared and UV/visible spectroscopy to identify those changes characteristic of pteridine chelation by a transition metal. Table VIII lists the prominent absorptions observed in the infrared spectra of the ligands and their cobalt bis chelates. Table IX lists data for the maxima observed in the electronic spectra of the cobalt complexes, the free ligands, and deprotonated ligands in dimethyl sulfoxide.

(18) Harding, M. M.; Long, H. A. *J. Chem. Soc. A* **1968**, 2554.

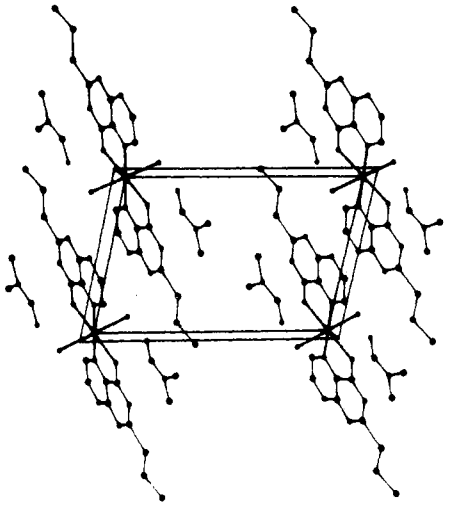

Figure 3. Packing diagram of $Co(ethp)_2(H_2O)_2 \cdot 2DMF$ viewed down the *a* axis showing stacking interactions between pteridine ligands.

Table IX. Electronic Spectral Data for Cobalt–Pteridine Complexes

ligand or complex	λ, nm (ε, M^{-1} cm^{-1})
ETHP	284 (21 300), 330 (11 500)
ETHP + (TEA)OH[a]	276 (30 600), 366 (10 400)
$Co(ethp)_2(H_2O)_2$	276 (18 900), 364 (10 400)
$Co(ethp)_2(imid)_2$	276 (22 600), 362 (12 400)
HMP	280 (7420), 354 (2680)
HMP + (TEA)OH	273 (15 000), 380 (3600)
$Co(hmp)_2(H_2O)_5 \cdot DMSO$	270 (23 000), 388 (10 900)
HP	272 (5620), 314 (7640)
HP + (TEA)OH	258 (14 900), 354 (9000)
$Co(hp)_2(H_2O)_4$	260 (14 300), 362 (7060)

[a] (TEA)OH is tetraethylammonium hydroxide, used as a 25% (w/w) methanolic solution.

Infrared spectroscopy proves to be an excellent tool for identifying pteridine chelation through the O_4 and N_5 atoms to a transition metal. Inspection of the data in Table VIII reveals that in each case the intense absorption of the carbonyl stretch in the 1650–1750-cm^{-1} region disappears on complexation. For pterins that have two distinct absorptions in the carbonyl region, one mode disappears and the second mode occurs with less intensity at lower energies. Data observed in this work for lumazine and its complex are identical with those reported previously.[15] A second diagnostic feature of infrared spectra of these pteridine complexes is the appearance of three intense absorptions in the region 1400–1600 cm^{-1}, due to mixed modes from C=C and C=N vibrations.[19] Each complex displays very strong bands near 1580, 1520, and 1500 cm^{-1}. These general features are also observed for pterin chelation by Mo(VI).

In Table IX the absorption maxima in the electronic spectra of the complexes and the free ligands are compared in the presence and absence of base in dimethyl sulfoxide. The results reported here point to the same conclusion reached by Jacobson et al.[6c] and by us in an earlier report.[13] The electronic spectra are dominated by ligand transitions, and no absorptions typical of d–d transitions can be discerned even in highly concentrated solutions. Comparisons between the spectra of solutions of the complexes and solutions of the free ligand in the presence of added base, tetraethylammonium hydroxide ((TEA)OH), indicate that solutions of the complexes have electronic absorptions characteristic of deprotonated pteridine. Solution conductivities of $Co(ethp)_2(H_2O)_2$ and $Co(ethp)_2(imid)_2$ in DMF solvent demonstrate that little dissociation occurs. Molar conductivities (Λ_M in units of Ω^{-1} cm^2 mol^{-1}) are 7.7 for $Co(ethp)_2(H_2O)_2$ and 8.7 for $Co(ethp)_2(imid)_2$ for 1.0 mM solutions. These values are well below the range established for 2:1 salts (Λ_M = 130–170) or 1:1 salts (Λ_M = 65–90) in DMF.[20] More dilute solutions (0.50 mM) had values of Λ_M = 22 and 8.4 for $Co(ethp)_2(H_2O)_2$ and $Co(ethp)_2(imid)_2$, respectively.

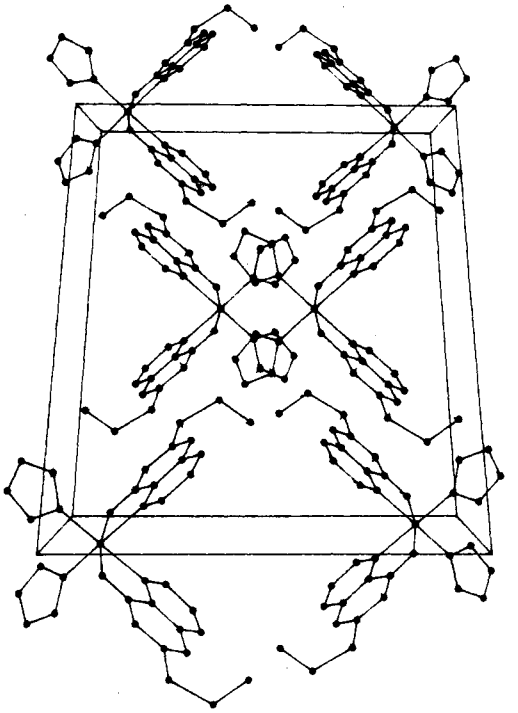

Figure 4. Packing diagram of $Co(ethp)_2(imid)_2$ viewed down the *a* axis.

Conclusion. The results reported in this work are potentially relevant to an understanding of pteridine cofactors that operate in the presence of transition-metal ions. The structures reported are the first for a first-row transition metal chelated to a pteridine core not possessing a fused benzo ring (e.g., of the isoalloxazine (flavin) type). As in the structures determined for transition-metal–alloxazine complexes, Co(II) prefers the coordination site at O_4 and N_5. Infrared spectroscopy is found to be a good diagnostic tool for detection of metal chelation at this site.[21] The isomerization resulting from imidazole substitution in this system also illustrates that variation in the coordination environment of a metal bound by histidine residues to a protein may alter pteridine–metal interactions.

Supplementary Material Available: Tables of bond angles, bond angles and bond lengths involving solvent atoms, atomic coordinates for hydrogen atoms, and close contacts involving hydrogen atoms in $Co(ethp)_2(H_2O)_2 \cdot 2dmf$, tables of bond angles, thermal parameters for solvent atoms, bond angles and bond lengths involving solvent atoms, and atomic coordinates for hydrogen atoms in $Co(ethp)_2(imid)_2$, and a table of elemental analysis data (Table II) (10 pages); tables of observed and calculated structure factors (19 pages). Ordering information is given on any current masthead page.

(19) Katritzky, A. R., Ed. *Physical Methods in Heterocyclic Chemistry*; Academic: New York, 1963; Vol. II.

(20) Geary, W. J. *Coord. Chem. Rev.* **1971**, *7*, 81.

(21) Related work in progress on low-valent Mo complexes of neutral pteridine ligands shows similar bands in the infrared spectra.